

SEEING ROADS THROUGH WORDS: A LANGUAGE-GUIDED FRAMEWORK FOR RGB-T DRIVING SCENE SEGMENTATION

Ruturaj Reddy^{*†§}, Hrishav Bakul Barua^{*⊗§}, Junn Yong Loo^{*}, Thanh Thi Nguyen[†], Ganesh Krishnasamy^{*}

^{*}School of Information Technology, Monash University Malaysia, Malaysia

[⊗]Robotics and Autonomous Systems Lab, TCS Research, Kolkata, India

[†]Faculty of Information Technology, Monash University, Australia

{ruturaj.reddy, hrishav.barua, loo.junnyong, thanh.nguyen9, ganesh.krishnasamy}@monash.edu

ABSTRACT

Robust semantic segmentation of road scenes under adverse illumination, lighting, and shadow conditions remain a core challenge for autonomous driving applications. RGB-Thermal fusion is a standard approach, yet existing methods apply static fusion strategies uniformly across all conditions, allowing modality-specific noise to propagate throughout the network. Hence, we propose CLARITY that dynamically adapts its fusion strategy to the detected scene condition. Guided by vision-language model (VLM) priors, the network learns to modulate each modality’s contribution based on the illumination state while leveraging object embeddings for segmentation, rather than applying a fixed fusion policy. We further introduce two mechanisms, *i.e.*, one which preserves valid dark-object semantics that prior noise-suppression methods incorrectly discard, and a hierarchical decoder that enforces structural consistency across scales to sharpen boundaries on thin objects. Experiments on the MFNet dataset demonstrate that CLARITY establishes a new state-of-the-art (SOTA), achieving 62.3% mIoU and 77.5% mAcc.

Index Terms— Image Segmentation, Autonomous Driving, VLM, CLIP, Hierarchical Fusion, RGB-Thermal Fusion.

1. INTRODUCTION

Semantic segmentation [1] is fundamental to robotic vision and autonomous driving safety [2], enabling precise identification of navigation elements [3]. While RGB-Thermal (RGB-T) fusion [4, 5] mitigates the illumination dependence of RGB-only methods, current frameworks face two limitations: **(a) Static fusion architectures:** Methods like CMX [6] and RTFNet [7] use fixed weights regardless of conditions, preventing aggressive suppression of noisy RGB branches (*e.g.*, at night); and **(b) Feature divergence:** Hierarchical decoders often suffer from divergence where coarse and fine features fail to converge [8], blurring thin objects.

[§]This research is supported by the Global Excellence and Mobility Scholarship (GEMS), Monash University (Australia & Malaysia).

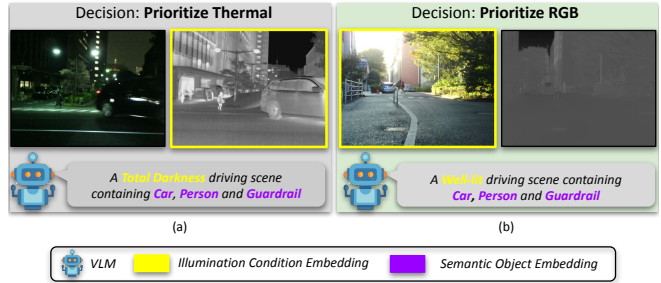


Fig. 1: VLM generates a template text caption for each scene, which is encoded into a semantic object embedding (words in **violet**) regardless of illumination conditions. (a) In poor illumination, the RGB image suffers from motion blur, obscuring the pedestrian. The thermal image remains clear. The VLM identifies this as a “Total Darkness” condition (words in **yellow**), activating kernels (*convolutional filters*) that prioritize thermal data to avoid integrating RGB noise. (b) Conversely, the RGB image provides clear details and edges for objects like the person and guardrail in “Well-lit” driving scene. The VLM gates the model to prioritize RGB over thermal input.

To address this, we propose CLARITY, a Language-Guided expert framework. Inspired by Language-Driven Restoration (LDR) [9], we utilize the Contrastive Language-Image Pre-training (CLIP) [10] based vision-language model (VLM) [11] to generate illumination condition and class-specific semantic object embeddings. Unlike static networks, our fusion module uses the illumination condition embedding to dynamically activate only the most relevant “Expert” kernel (*e.g.*, a “Night Expert” prioritizing thermal features), while semantic object embedding serves as semantic priors for ambiguous targets (see Fig. 1). We also transfer the Self-Calibrated Illumination (SCI) framework [8] into the decoder to enforce consistency.

Early RGB-T approaches such as MFNet [12] and recent Transformer-based methods such as MMSMCNet [13] remain “condition-agnostic,” applying uniform fusion logic regardless of severity. We advance this by introducing

condition-specific dynamic gating inspired by the Mixture-of-Experts (MoE) approach. Recent works, such as CA-Fuser [14], use text tokens to guide fusion. We extend this paradigm to RGB-T segmentation, using embeddings to dynamically gate the fusion and teaching the network to prioritize thermal features when prompts indicate conditions such as “Total Darkness.” Unlike static layers, this semantic gating recalibrates feature importance layer-by-layer, preventing noise contamination during critical safety scenarios. Novel priors from low-light enhancement remain underutilized. We address this by adapting SCI [8] to eliminate structural artifacts in objects. We use “unbalanced point transformer prior” from UPT-Flow [15] to flag distorted RGB pixels, ensuring robustness against illumination variations. Our **key contributions** are as follows:

- **Language-Guided Dynamic Fusion:** We propose an RGB-T segmentation network that utilizes CLIP-derived semantic prompts to gate a Sparse MoE [9] based on illumination conditions, while simultaneously integrating object embeddings to guide segmentation.
- **Soft-Gated Unbalanced Attention:** We introduce a “Soft” unbalanced point mechanism [15] that identifies distorted RGB pixels via variance mapping. Unlike hard-thresholding methods that blind the model to dark objects, our soft-gating preserves critical color cues (e.g., Traffic Cones) while suppressing noise.
- **Self-Calibrated Decoding:** We design the self-calibration module based on illumination learning [8] to bridge the decoder stages, significantly reducing boundary artifacts and achieving SOTA on overall metrics.

2. METHOD

2.1. Architectural Overview of CLARITY

The proposed framework for training (Fig. 2) adopts a dual-stream structure via three restoration-based mechanisms for fusion. Specifically, the encoder integrates a Language-Guided MoE that utilizes semantic prompts to gate glare-affected pixels to thermal experts and inject object embeddings. This is complemented by a Soft-Gated Unbalanced Point Transformer (SG-UPT) to preserve faint details in low-confidence regions, while a Self-Calibrated Decoder enforces inter-stage feature consistency to prevent modality conflict.

2.2. Feature Extraction and Semantic Conditioning

VLMs are becoming increasingly popular in guiding low-level vision tasks such as Language-Driven Restoration (LDR) [9]. In their work, CLIP detects weather degradations to activate specific noise-removal kernels. We use CLIP-based VLM to extract a *Illumination Condition Embedding* P_{cond} for gating the fusion process and a *Holistic*

Scene Embedding (consisting of both illumination condition and semantic object embeddings) P_{emb} for semantic scene understanding. Given an RGB image $I_{RGB} \in \mathbb{R}^{H \times W \times 3}$ and a thermal image $I_{Th} \in \mathbb{R}^{H \times W \times 1}$, we finetune two pretrained ConvNeXt [16] networks to extract hierarchical feature maps $\{F_{RGB}^i, F_{Th}^i\}_{i=1}^4$. Simultaneously, to capture the nuance of the driving environment, we generate a comprehensive prompt T_p given an input I_{RGB} to interrogate the scene context. Crucially, to ensure strict semantic alignment with the downstream segmentation task, we define fixed constraints for both illumination conditions and objects detected within the prompt. First, we establish a set of distinct illumination conditions C_{cond} consisting of: *Glare, Well-lit, Overcast, Twilight, and Total Darkness*. Second, we constrain object descriptors to the pre-defined MFNet [17] class set C_{target} , including: *Car, Person, Bike, Curve, Car Stop, Guardrail, Color Cone, and Bump*. The prompt T_p is therefore constructed textually as:

$$\text{“A } \underbrace{\langle \text{condition} \rangle}_{\{\text{Glare, Well-lit, Overcast, etc.}\}} \text{ driving scene containing } \underbrace{\langle O_{detected} \rangle}_{\{\text{Car, Person, Bike, etc.}\}} \text{”, (1)}$$

where, the chosen $\langle \text{condition} \rangle \in C_{cond}$, and the detected objects $\langle O_{detected} \rangle \subseteq C_{target}$ (an example caption T_c generated - “A **Total Darkness** driving scene containing **Car, Person** and **Guardrail**”, see Figs. 1 and 2). By filtering the VLM output to strictly match these targeted sets, we not only prevent open-vocabulary noise from corrupting the condition vector but also gain a significant advantage in detecting challenging objects. Classes such as ‘Guardrail’ are often visually ambiguous or obscure in MFNet images due to poor illumination. By explicitly querying CLIP based on its vast pre-trained semantic knowledge, we inject a strong, task-specific prior into the system. This ensures the fusion process is heavily biased towards features relevant to these hard-to-find classes, rather than just dominant background elements.

The caption T_c begins with the illumination condition phrase T_i (e.g., “A **Total Darkness** driving scene”). Acting as a Task-Aligned Global Controller, T_i directs the MoE fusion to activate $Top-K$ experts ($K=2$). We encode T_i (P_{cond}) using a frozen CLIP encoder followed by a Multilayer Perceptron (MLP) for alignment. Similarly, the complete caption T_c is processed through the same pipeline to yield P_{emb} , an embedding that encodes both the illumination condition and specific semantic classes (e.g., Guardrail):

$$P_{cond} = \text{MLP}(\text{CLIP}_{enc}(T_i)), \quad P_{cond} \in \mathbb{R}^C, \quad (2)$$

$$P_{emb} = \text{MLP}(\text{CLIP}_{enc}(T_c)), \quad P_{emb} \in \mathbb{R}^C, \quad (3)$$

where C denotes the channel dimensionality of the encoder feature maps.

2.3. Soft-Gated Unbalanced Point Attention (SG-UPT)

The Unbalanced Point Prior (UPT) [15] is originally introduced for low-light image enhancement, employing a hard

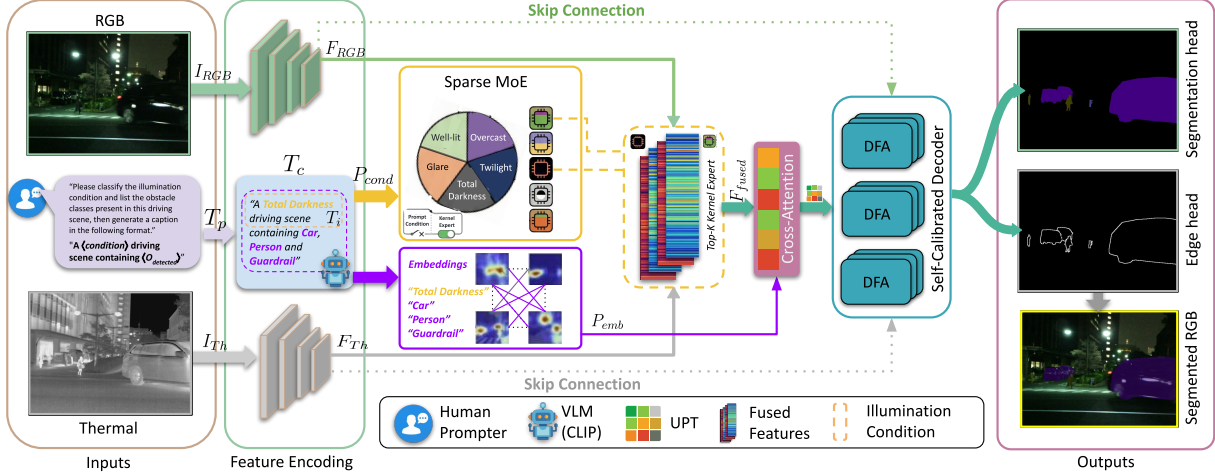


Fig. 2: Architecture of the proposed CLARITY method. The framework begins with a Semantic Condition Generator, where a VLM (CLIP) analyzes the scene to generate caption T_c . This process yields two key embeddings, *i.e.*, an illumination condition embedding (P_{cond}) from T_c derived for illumination conditions ($\langle \text{condition} \rangle$) and a holistic scene embedding (P_{emb}) derived from T_c for detected objects ($\langle O_{detected} \rangle$) and illumination condition. P_{cond} serves as a gating signal for the Sparse MoE, dynamically routing inputs to degradation-specific Top- K Kernel Experts for adaptive fusion. The fused features are then enhanced by a Soft-Gated UPT to recover faint thermal details. Finally, a Self-Calibrated Decoder with Dilated Feature Aggregation (DFA) blocks captures multi-scale context before feeding the Segmentation and Edge Heads.

threshold ($T = 0.1$) on RGB ratios to binary mask out pixels with severe color distortion. We identify that such hard-thresholding is detrimental to segmentation as it creates binary gradient blockers that sever the semantic signal of valid dark objects (*e.g.*, traffic cones). Therefore, we propose a *Soft-Gated Tanh Bias*. First, we design the Unbalanced Map $M_{un} \in \mathbb{R}^{H \times W}$ to capture the specific artifacts of driving scenes (*e.g.*, noise and underexposure) rather than the color ratio. We formulate M_{un} based on local variance and intensity:

$$M_{un} = \sigma_{\text{local}}(I_{RGB}) + (1 - \mu_{\text{local}}(I_{RGB})), \quad (4)$$

where σ_{local} and μ_{local} denote local variance and mean pooling operations, respectively. This map highlights regions with high noise (high variance) or extreme darkness (low mean).

Second, we inject this map into the attention mechanism as a soft bias rather than a hard mask. Let $Q, K, V \in \mathbb{R}^{N \times d}$ be the projections of the flattened feature map $X \in \mathbb{R}^{N \times C}$ (where $N = H \times W$). The refined feature \hat{X} is computed as:

$$\hat{X} = \text{Softmax} \left(\frac{QK^T}{\sqrt{d}} - \lambda \cdot \tanh(M_{un}^{\text{flat}}) \right) V, \quad (5)$$

where $M_{un}^{\text{flat}} \in \mathbb{R}^{1 \times N}$ is the flattened and broadcasted map, λ is a learnable scalar, and d is the channel dimension of the query/key projections, serving as a scaling factor to prevent gradient saturation in the Softmax operation. The tanh term softly down-weights the attention scores for noisy or glare-affected pixels (where M_{un} is high), effectively suppressing their contribution to the global context without completely discarding their features.

2.4. Language-Guided Sparse MoE Fusion

To achieve illumination condition-specific modality integration, we propose a Language-Guided Sparse (MoE) for dynamic feature fusion. Drawing inspiration from the degradation-adaptive routing in LDR [9], we replace standard static fusion layers with a routable expert bank that reconfigures based on semantic context. We maintain N convolution filters $E = \{E_1, \dots, E_N\}$ and denote them as expert kernels. A gating network W_g projects the condition vector embedding P_{cond} and input features into a selection score S :

$$S = \text{Softmax}(W_g([F_{RGB}, F_{Th}, \text{Expand}(P_{cond})])), \quad (6)$$

where $\text{Expand}(\cdot)$ broadcasts the global condition vector P_{cond} to the spatial dimensions $H \times W$ and $[\cdot]$ denotes concatenation and $S \in \mathbb{R}^{H \times W \times N}$ represents the gating weights. The fused feature F_{fused} is the weighted summation of the Top- K experts applied to the concatenated input features. Let $\rho(k)$ denote the index of the k^{th} highest scoring expert at a given pixel. The sparse aggregation is formulated as:

$$F_{\text{fused}} = \sum_{k=1}^K S_{\rho(k)} \odot E_{\rho(k)}([F_{RGB}, F_{Th}]), \quad (7)$$

where $S_{\rho(k)} \in \mathbb{R}^{H \times W}$ is the spatial confidence map for the chosen expert $E_{\rho(k)}$. This mechanism allows the network to physically reconfigure per-pixel, activating the ‘‘Thermal Expert’’ only at specific coordinates where glare or darkness is detected. Finally, we employ a standard cross-attention between F_{fused} and P_{emb} to inject holistic semantic scene context into the spatial features.

Table 1: Comparison of semantic segmentation results on the MFNet dataset [5]. Best results are in **bold**.

| Methods | Car | | Person | | Bike | | Curve | | Carstop | | Guardrail | | Cone | | Bump | | mAcc(%) | mIoU(%) |
|---|-------------|-------------|-------------|-------------|-------------|-------------|-------------|-------------|-------------|-----------|-------------|-------------|-------------|-------------|-------------|-------------|-------------|-------------|
| | Acc | IoU | Acc | IoU | Acc | IoU | Acc | IoU | Acc | IoU | Acc | IoU | Acc | IoU | Acc | IoU | | |
| FuseSeg (<i>TASE'21</i>) [18] | 93.1 | 87.9 | 81.4 | 71.7 | 78.5 | 64.6 | 68.4 | 44.8 | 29.1 | 22.7 | 63.7 | 6.4 | 55.8 | 46.9 | 66.4 | 47.9 | 70.6 | 54.5 |
| GMNet (<i>TIP'21</i>) [19] | 94.1 | 86.5 | 83 | 73.1 | 76.9 | 61.7 | 59.7 | 44 | 55 | 42.3 | 71.2 | 14.5 | 54.7 | 48.7 | 73.1 | 47.4 | 74.1 | 57.3 |
| MFNet (<i>IROS'17</i>) [12] | 95.1 | 87.9 | 85.2 | 66.8 | 83.9 | 64.4 | 64.3 | 47.1 | 50.8 | 36.1 | 45.9 | 8.4 | 62.8 | 55.5 | 73.8 | 62.2 | 74.7 | 57.3 |
| RTFNet (<i>RAL'19</i>) [7] | 93.0 | 87.4 | 79.3 | 70.3 | 76.8 | 62.7 | 60.7 | 45.3 | 38.5 | 29.8 | 0.0 | 0.0 | 45.5 | 29.1 | 74.7 | 55.7 | 63.1 | 53.2 |
| DooDLeNet (<i>CVPRW'22</i>) [20] | 91.7 | 86.7 | 81.3 | 72.2 | 76.6 | 62.5 | 58.9 | 46.7 | 36.2 | 28 | 35.2 | 5.1 | 56.9 | 50.7 | 74.8 | 65.8 | 67.9 | 57.3 |
| Parameter Sharing (<i>TITS'24</i>) [21] | 94.3 | 88.3 | 82.8 | 72.5 | 82.9 | 65.2 | 74.9 | 46.6 | 62.7 | 47 | 42.7 | 11.6 | 55 | 46 | 76 | 57.1 | 74.4 | 59.1 |
| EGFNet (<i>TITS'24</i>) [5] | 95.8 | 87.6 | 89.0 | 69.8 | 80.6 | 58.8 | 71.5 | 42.8 | 48.7 | 33.8 | 33.6 | 7.0 | 65.3 | 48.3 | 71.1 | 47.1 | 72.7 | 54.8 |
| IGFNet (<i>ROBIO'23</i>) [22] | 93.2 | 88.0 | 83.4 | 74.0 | 71.8 | 62.7 | 67.6 | 48.2 | 45.4 | 36.0 | 68.5 | 14.2 | 58.4 | 52.4 | 68.3 | 57.5 | 72.9 | 59.0 |
| MMSMCNet (<i>TCSV'T'23</i>) [13] | 96.2 | 89.2 | 93.2 | 69.1 | 83.4 | 63.5 | 74.4 | 46.4 | 56.6 | 41.9 | 26.9 | 8.8 | 70.2 | 48.8 | 77.5 | 57.6 | 75.2 | 58.1 |
| CMX(MiT-B2)* (<i>TITS'23</i>) [6] | 93.8 | 89.4 | 84.6 | 74.8 | 75.6 | 64.7 | 64.4 | 47.3 | 42.5 | 30.1 | 54.8 | 8.1 | 54.1 | 52.4 | 72.2 | 59.4 | 71.29 | 58.2 |
| CMX(MiT-B4) (<i>TITS'23</i>) [6] | - | 90.1 | - | 75.2 | - | 64.5 | - | 50.2 | - | 35.3 | - | 8.5 | - | 54.2 | - | 60.6 | - | 59.7 |
| CMAAHF (<i>ICIP'25</i>) [4] | 96.3 | 91.2 | 83.7 | 74.1 | 82.6 | 66.6 | 73.8 | 46.1 | 64.1 | 43.8 | 47.1 | 18.2 | 67.1 | 56.1 | 78.9 | 60.7 | 76.3 | 61.9 |
| CLARITY (Ours) | 97.4 | 91.5 | 86.0 | 74.8 | 84.8 | 67.2 | 76.2 | 46.6 | 66.3 | 44.3 | 49.3 | 18.7 | 66.2 | 55.7 | 78.2 | 60.1 | 77.5 | 62.3 |

*Reproduced using model checkpoint.

2.5. Self-Calibrated Hierarchical Decoder

Inspired by the Self-Calibrated Illumination (SCI) framework [8], which enforces exposure stability via weight sharing, we design a task-specific variant to alleviate feature divergence in hierarchical decoding. In standard decoders, error accumulation across upsampling stages often blurs the boundaries of small objects. To prevent this, we implant a self-calibrator to anchor the decoding trajectory.

Let D_t be the decoder feature at stage t . We utilize a parameter-sharing decoding block \mathcal{H}_θ instantiated as a Dilated Feature Aggregation (DFA) module. The DFA block [4] applies parallel convolutions with varying dilation rates to capture multi-scale context without resolution loss. Drawing on the convergence property of SCI, we force the output of the subsequent stage D_{t+1} to be calibrated against the initial structural representation D_1 :

$$D_{t+1} = \mathcal{H}_\theta(\text{Up}(D_t) + \mathcal{S}_\phi(D_1)), \quad (8)$$

where $\text{Up}(\cdot)$ denotes bilinear upsampling and \mathcal{S}_ϕ acts as a learnable calibrator. This formulation ensures that the DFA blocks remain centered around the fixed initial estimate D_1 rather than drifting due to cascading dependencies. Here, \mathcal{S}_ϕ acts as a learnable calibrator that projects the coarse semantic anchor D_1 to match the resolution of stage t . This explicitly suppresses the “error clusters” around high-frequency edges, allowing multi-scale DFA features to sharpen the boundaries of thin structures such as guardrails.

2.6. Edge-Aware Loss Function

To resolve the severe class imbalance between edge and non-edge pixels, we employ a joint loss combining Weighted Cross-Entropy (\mathcal{L}_{seg}) for semantic segmentation and Focal Loss (\mathcal{L}_{edge}) for the auxiliary edge head. The total objective is formulated as:

$$\mathcal{L}_{total} = \mathcal{L}_{seg}(P, G) + \beta \mathcal{L}_{edge}(P_e, G_e), \quad (9)$$

where P, G and P_e, G_e denote the semantic and edge predictions and ground truths, respectively. We empirically set $\beta = 0.6$ to balance the auxiliary task gradient.

3. EXPERIMENTS AND RESULTS

Implementation: We implement our method using PyTorch, trained on an Nvidia A40 GPU (48GB VRAM), utilizing the AdamW optimizer and a poly learning rate schedule.

Datasets: We evaluate on the popular MFNet dataset [5], comprising 1,569 aligned RGB-T pairs (480×640) captured in urban scenes via an *InReC R500* camera. Following standard protocols [7], the data is split into 784 training, 392 validation, and 393 testing images. The dataset annotates nine classes: one background and eight obstacles (*e.g.*, *Car*, *Guardrail*). A critical challenge is the severe “long-tail” imbalance where objects like *Color Cones* are rare, necessitating our weighted loss formulation. Furthermore, while the metadata distinguishes 820 daytime and 749 nighttime images, we find these binary labels insufficient to capture sensor degradations, motivating the detailed categorization in methodology.

Methods: To validate the superiority of our method, we benchmark against representative state-of-the-art methods. We compare with CNN-based fusion networks including MFNet [12], RTFNet [7], and EGFNet [5], which utilize dual-stream encoders. Additionally, we compare against recent Transformer-based approaches such as CMX [6], which employs cross-modal fusion, and CMAAHF [4], which utilizes hierarchical attention.

Quantitative Results. Table 1 compares performance on the MFNet test set [5]. While the CMX baseline fragments thin structures like *Guardrails* (8.1% IoU) and misses *Color Cones* due to weak thermal signatures, CLARITY utilizes Soft-Gated UPT to explicitly recover these details, boosting *Guardrail* IoU to 18.7%. Our CLIP-generated prompts provide semantic priors that enable the detection of objects barely visible in both modalities, yielding continuous masks and raising *Car* IoU to 91.5% compared to 89.4% for CMX. CLARITY sets a new state-of-the-art with 62.3% mIoU and 77.5% mAcc, surpassing CMAAHF (61.9% mIoU). This performance advantage extends to dynamic classes such as *Bike* (67.2% IoU), confirming that our semantic gating effectively handles both static structural elements and moving obstacles better than standard fusion baselines.

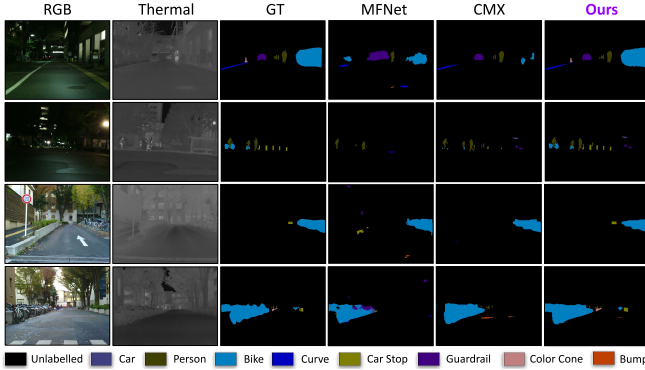


Fig. 3: Segmented results generated by the proposed CLARITY and state-of-the-art methods on MFNet dataset [5].

Table 2: Component Contribution Analysis on the MFNet dataset. We evaluate the incremental impact of the Sparse Mixture-of-Experts (MoE), the Language-Driven Gating and scene embedding via CLIP, and the Soft-Gated UPT (SG-UPT) on the baseline Dual-Stream architecture.

| Model Configuration | mIoU (%) |
|-------------------------------|--------------------|
| Baseline (Dual ConvNeXt [16]) | 56.5 |
| + Sparse MoE (Random Router) | 57.7 (+1.2) |
| + $CLIP_{P_{cond}}$ | 60.1 (+2.4) |
| + $CLIP_{P_{emb}}$ | 61.0 (+0.9) |
| + Soft-Gated UPT | 62.3 (+1.3) |

Qualitative Results: Fig. 3 presents a qualitative comparison on the MFNet test set [5]. While CMX provides a strong baseline, it exhibits structural fragmentation on thin objects (*e.g.*, guardrails) and frequently fails to detect Color Cones, often misclassifying them as background due to their limited thermal footprint. In contrast, CLARITY utilizes the Soft-Gated UPT via VLM gating to explicitly recover these faint details. Notably, the integration of CLIP-generated prompts enables our model to detect objects barely visible in both RGB and thermal modalities by leveraging semantic priors (*embeddings*) where visual cues are insufficient. This yields significantly sharper boundaries and complete masks compared to the coarser, fragmented predictions of MFNet.

Ablation Study: We investigate the impact of the MoE architecture and the Language-Driven Gating and embedding. As shown in Table 2, replacing the standard decoder with a “Random Router” MoE provides only marginal gains (+1.2%). However, enabling CLIP Gating via P_{cond} , which

Table 3: Comparison of Attention Gating Mechanisms. We compare the original UPT hard thresholding ($T = 0.1$) against our proposed Soft Tanh modulation.

| Mechanism | Gating Function | mIoU(%) |
|-------------------|---------------------------------|--------------------|
| No Prior | - | 60.1 |
| Original UPT [15] | Hard Cut ($P < 0.1$) | 60.5 (+0.4) |
| SG-UPT (Ours) | Soft Tanh ($\tanh(\alpha P)$) | 62.3 (+1.8) |

Table 4: Impact of Semantic Prompt Granularity. Fine-grained illumination conditions allow experts to specialize in specific degradations as compared to binary labels only.

| Prompt Strategy | Condition Set (C_{cond}) | mIoU (%) |
|---------------------|---|--------------------|
| No Prompt (w/o VLM) | - | 57.7 |
| Binary Labels | {Day, Night} | 59.2 (+1.5) |
| Ternary Labels | {Day, Overcast, Night} | 60.5 (+1.3) |
| Fine-Grained (Ours) | {Glare, Well-lit, Overcast, Twilight, Total Darkness} | 62.3 (+1.8) |

allows the model to select experts based on the prompt, yields a significant boost to 60.1% mIoU. Then the introduction of CLIP-generated scene embedding P_{emb} increases the performance further to 61.0%. The final addition of the Soft-Gated UPT pushes performance to 62.3%, confirming that semantic routing and detailed feature preservation are complementary.

We validate our modification to the Unbalanced Point Transformer (UPT). The original UPT uses a hard threshold ($T=0.1$) to filter distorted pixels. As shown in Table 3, this hard cut suppresses faint objects like Guardrails (13.1% IOU). Our proposed Soft Tanh gating preserves gradients for these low-light pixels, improving Guardrail recovery by over 5%.

Finally, we analyze prompt engineering for the gating mechanism. Table 4 demonstrates that using the dataset’s native binary labels (“Day”, “Night”) is insufficient (59.2% mIoU) because “Night” conflates distinct degradation modes like pitch darkness and headlight glare. Similarly, we observe only a minute improvement with ternary labels (“Day”, “Overcast”, “Night”). Finally, our fine-grained 5-condition stratum allows the MoE to specialize kernels for these specific noise distributions, achieving optimal results.

4. CONCLUSIONS

In this work, we introduce a dynamic fusion framework designed to address the vulnerability of static RGB-T networks under varying illumination conditions. By integrating a semantic gating mechanism driven by fine-grained prompts, our model dynamically routes pixels to degradation-specific experts, significantly outperforming coarser binary or ternary conditioning strategies. Furthermore, the proposed SG-UPT resolves the feature-suppression issue inherent to hard-thresholding priors, enabling recovery of faint, safety-critical objects such as guardrails and color cones in low-light scenarios. Extensive evaluations on the MFNet benchmark demonstrate that our approach establishes a new state-of-the-art with 62.3% mIoU and 77.5% mAcc, outperforming recent Transformer-based methods such as CMX and CMAAHF. These results confirm that injecting semantic condition awareness into the fusion process is a key factor for robust autonomous perception. Future work will focus on extending this approach to adverse weather scenarios (*i.e.*, foggy, rainy, snowy, *etc.*) to enhance the diversity of kernel experts via VLM gating.

5. REFERENCES

- [1] Liang-Chieh Chen, George Papandreou, Iasonas Kokkinos, Kevin Murphy, and Alan L. Yuille, “Deeplab: Semantic image segmentation with deep convolutional nets, atrous convolution, and fully connected crfs,” *IEEE Transactions on Pattern Analysis and Machine Intelligence*, vol. 40, no. 4, pp. 834–848, 2018.
- [2] Di Feng, Ali Harakeh, Steven L. Waslander, and Klaus Dietmayer, “A review and comparative study on probabilistic object detection in autonomous driving,” *IEEE Transactions on Intelligent Transportation Systems*, vol. 23, no. 8, pp. 9961–9980, 2022.
- [3] Federico Nesti, Giulio Rossolini, Saasha Nair, Alessandro Biondi, and Giorgio Buttazzo, “Evaluating the robustness of semantic segmentation for autonomous driving against real-world adversarial patch attacks,” in *Proceedings of the IEEE/CVF Winter Conference on Applications of Computer Vision (WACV)*, January 2022, pp. 2280–2289.
- [4] Saheli Hazra and Ujjwal Bhattacharya, “Cross-modal attention with adaptive and hierarchical fusion for robust rgb-t image segmentation for safe driving,” in *2025 IEEE International Conference on Image Processing (ICIP)*. IEEE, 2025, pp. 2139–2144.
- [5] Shaohua Dong, Wujie Zhou, Cai Xu, and Weiqing Yan, “Egfn: Edge-aware guidance fusion network for rgb-thermal urban scene parsing,” *IEEE Transactions on Intelligent Transportation Systems*, vol. 25, no. 1, pp. 657–669, 2024.
- [6] Jiaming Zhang, Huayao Liu, Kailun Yang, Xinxin Hu, Ruiping Liu, and Rainer Stiefelhagen, “Cmx: Cross-modal fusion for rgb-x semantic segmentation with transformers,” *IEEE Transactions on Intelligent Transportation Systems*, vol. 24, no. 12, pp. 14679–14694, 2023.
- [7] Yuxiang Sun, Weixun Zuo, and Ming Liu, “Rtfnet: Rgb-thermal fusion network for semantic segmentation of urban scenes,” *IEEE Robotics and Automation Letters*, vol. 4, no. 3, pp. 2576–2583, 2019.
- [8] Long Ma, Tengyu Ma, Chengpei Xu, Jinyuan Liu, Xin Fan, Zhongxuan Luo, and Risheng Liu, “Learning with self-calibrator for fast and robust low-light image enhancement,” *IEEE Transactions on Pattern Analysis and Machine Intelligence*, vol. 47, no. 10, pp. 9095–9112, 2025.
- [9] Hao Yang, Liyuan Pan, Yan Yang, and Wei Liang, “Language-driven all-in-one adverse weather removal,” in *2024 IEEE/CVF Conference on Computer Vision and Pattern Recognition (CVPR)*, 2024, pp. 24902–24912.
- [10] Alec Radford, Jong Wook Kim, Chris Hallacy, Aditya Ramesh, Gabriel Goh, Sandhini Agarwal, Girish Sastry, Amanda Askell, Pamela Mishkin, Jack Clark, et al., “Learning transferable visual models from natural language supervision,” in *International conference on machine learning*. PMLR, 2021, pp. 8748–8763.
- [11] Xingcheng Zhou, Mingyu Liu, Ekim Yurtsever, Bare Luka Zagar, Walter Zimmer, Hu Cao, and Alois C Knoll, “Vision language models in autonomous driving: A survey and outlook,” *IEEE Transactions on Intelligent Vehicles*, 2024.
- [12] Qishen Ha, Kohei Watanabe, Takumi Karasawa, Yoshitaka Ushiku, and Tatsuya Harada, “Mfnet: Towards real-time semantic segmentation for autonomous vehicles with multi-spectral scenes,” in *2017 IEEE/RSJ International Conference on Intelligent Robots and Systems (IROS)*. IEEE, 2017, pp. 5108–5115.
- [13] Wujie Zhou, Han Zhang, Weiqing Yan, and Weisi Lin, “Mmsmcnet: Modal memory sharing and morphological complementary networks for rgb-t urban scene semantic segmentation,” *IEEE Transactions on Circuits and Systems for Video Technology*, vol. 33, no. 12, pp. 7096–7108, 2023.
- [14] Tim Brödermann, Christos Sakaridis, Yuqian Fu, and Luc Van Gool, “Cafuser: Condition-aware multimodal fusion for robust semantic perception of driving scenes,” *IEEE Robotics and Automation Letters*, vol. 10, no. 4, pp. 3134–3141, 2025.
- [15] Lintao Xu, Changhui Hu, Yin Hu, Xiaoyuan Jing, Ziyun Cai, and Xiaobo Lu, “Upt-flow: Multi-scale transformer-guided normalizing flow for low-light image enhancement,” *Pattern Recognition*, vol. 158, pp. 111076, 2025.
- [16] Zhuang Liu, Hanzi Mao, Chao-Yuan Wu, Christoph Feichtenhofer, Trevor Darrell, and Saining Xie, “A convnet for the 2020s,” in *Proceedings of the IEEE/CVF Conference on Computer Vision and Pattern Recognition (CVPR)*, June 2022, pp. 11976–11986.
- [17] Qishen Ha, Kohei Watanabe, Takumi Karasawa, Yoshitaka Ushiku, and Tatsuya Harada, “Mfnet: Towards real-time semantic segmentation for autonomous vehicles with multi-spectral scenes,” in *2017 IEEE/RSJ International Conference on Intelligent Robots and Systems (IROS)*, 2017, pp. 5108–5115.
- [18] Yuxiang Sun, Weixun Zuo, Peng Yun, Hengli Wang, and Ming Liu, “Fuseseg: Semantic segmentation of urban scenes based on rgb and thermal data fusion,” *IEEE Transactions on Automation Science and Engineering*, vol. 18, no. 3, pp. 1000–1011, 2021.
- [19] Wujie Zhou, Jinfu Liu, Jingsheng Lei, Lu Yu, and Jenq-Neng Hwang, “Gmnet: Graded-feature multilabel-learning network for rgb-thermal urban scene semantic segmentation,” *IEEE Transactions on Image Processing*, vol. 30, pp. 7790–7802, 2021.
- [20] Oriel Frigo, Lucien Martin-Gaffe, and Catherine Wacongne, “Doodlenet: Double deeplab enhanced feature fusion for thermal-color semantic segmentation,” in *Proceedings of the IEEE/CVF Conference on Computer Vision and Pattern Recognition (CVPR) Workshops*, June 2022, pp. 3021–3029.
- [21] Guofa Li, Yongjie Lin, Delin Ouyang, Shen Li, Xiao Luo, Xingda Qu, Dawei Pi, and Shengbo Eben Li, “A rgb-thermal image segmentation method based on parameter sharing and attention fusion for safe autonomous driving,” *IEEE Transactions on Intelligent Transportation Systems*, vol. 25, no. 6, pp. 5122–5137, 2024.
- [22] Haotian Li and Yuxiang Sun, “Igfn: Illumination-guided fusion network for semantic scene understanding using rgb-thermal images,” in *2023 IEEE International Conference on Robotics and Biomimetics (ROBIO)*, 2023, pp. 1–6.